AMORPHOUS SILICON X-RAY IMAGE SENSOR

J. Chabbal, C. Chaussat, T. Ducourant, L. Fritsch, J. Michaïlos,
V. Spinnler, G. Vieux, M. Arques *
Thomson Tubes Electroniques, 38430 Moirans, France

G. Hahm, M. Hoheisel, H. Horbaschek, R. Schulz, M. Spahn
Siemens AG, Medical Engineering, 91052 Erlangen, Germany

ABSTRACT

The design and the performance of a 20 cm x 20 cm flat panel X-ray detector for digital radiography and fluoroscopy is described : Thin film amorphous silicon (aSi) technology has been used to build a 1024 x 1024 photodetector matrix, each pixel including both a photodiode and a switching diode ; the pixel size is 196 x 196 μm^2. A high resolution and high absorption CsI(Tl) scintillator layer covers the top of the photodetector matrix in order to provide for X-ray to light conversion. For low electronic noise and 30 fr/s operating rate we developed a custom design charge readout integrated circuit. The detector delivers a 12 bit digital output.

The image quality, signal to noise ratio and DQE are presented and discussed. The flat panel detector provides a MTF in excess of 30 % at 2 lp/mm and a high contrast ratio without any distortion on the whole imaging area. The X-ray absorption is 70% for 50 KeV photons. The readout amplifier is optimized to reduce the electronic noise down to 1000 e-. This low noise level, combined with high sensitivity (1150 e-/incident X-ray quantum) provides the capability for fluoroscopic applications.

The digital flat panel detector has been integrated in a C-arm system for cardiology and has been used on a regular basis in a European hospital since february 1995. The results are discussed for several operating modes : radiography and fluoroscopy.

Conclusions on present detector performances, as well as further improvements, are presented.

Keywords : aSi, a-Si:H, array, image sensor, pixel.

1. INTRODUCTION

Driven by the large and rapidly expanding active matrix LCD market, the successful development of large area thin film amorphous silicon processes over the last decades has made available suitable technology for the fabrication of solid-state image sensor arrays for X-ray imaging. Many publications have been reported for document reproduction and medical imaging applications : they are all based on 2D matrixes consisting of an aSi photodiode as the light sensing element, and an aSi switching device ; this device can be a thin film transistor (TFT) [1,2,3,4] or more simply, a thin film diode (TFD) [5,6,7].

The motivation driving such developments is the replacement of both X-ray film for radiographic applications, and conventional X-ray Image Intensifier TV (XRII-TV) systems for fluoroscopic X-ray imaging.

In the field of fluoroscopic X-ray imaging, the advantages of the new technology are numerous :

- Excellent large area (coarse) contrast, compared to XRII-TV based systems,
- No geometrical distortion (due to the magnetic field on the earth) when a movement of the detector is needed,
- No distortion at the edges, as in conventional XRII based systems,
- New potential applications thanks to zero image distortion : angiography, double energy radiography, 3D imaging..
- Homogeneous resolution (easier and more precise digital processing algorithm), built-in spatial quantization,
- Flatness and compactness ($\sim$1/4 of the thickness of equivalent current XRII) ; lighter and more handy systems ; radiation protection chambers can be kept compact in industrial systems ; possible realization of very compact X-ray systems (radioscopy, CT, laminography, digital tomosynthesis) for integration in production lines.
- Mixed fluoroscopic/radiographic applications with immediate switching.

* now with LETI, Grenoble, France

0-8194-2083-2/96/$6.00

For radiographic X-ray imaging, additional advantages are at hand :

- High sensitivity and thus, possible dose reduction,
- Real time imaging, instantaneous access to the image,
- Ease of operation : no cassette to be handled anymore,
- Direct transmission of images to digital storage devices ; connection to PACS networks or display on remote workstations.

In the field of fluoroscopic X-ray imaging, few results have been published so far [1] ; none deal with the combination of large area, small pixel size, and fluoroscopic performances ; In this framework, this paper presents the development of a 20 cm x 20 cm X-ray image detector ; as with fluoroscopic imaging, the achievable S/N ratio is the key figure, we describe the various noise sources as well as further improvements expected in the future.

2. DETECTOR DESCRIPTION

The flat panel sensor consists of an active 1024 x 1024 matrix, built in the so-called Double Diode technology (2xD), which means that the two diodes are deposited separately (as opposed to Single Layer Diode technology (SLD) where both diodes are deposited at the same time) ; each 196 x 196 μm^2 pixel is made up of an aSi photodiode (pD) in series with an aSi switching diode (sD); the array is matrix-addressed via lines for the row selection and via columns for the charge readout (Fig1).

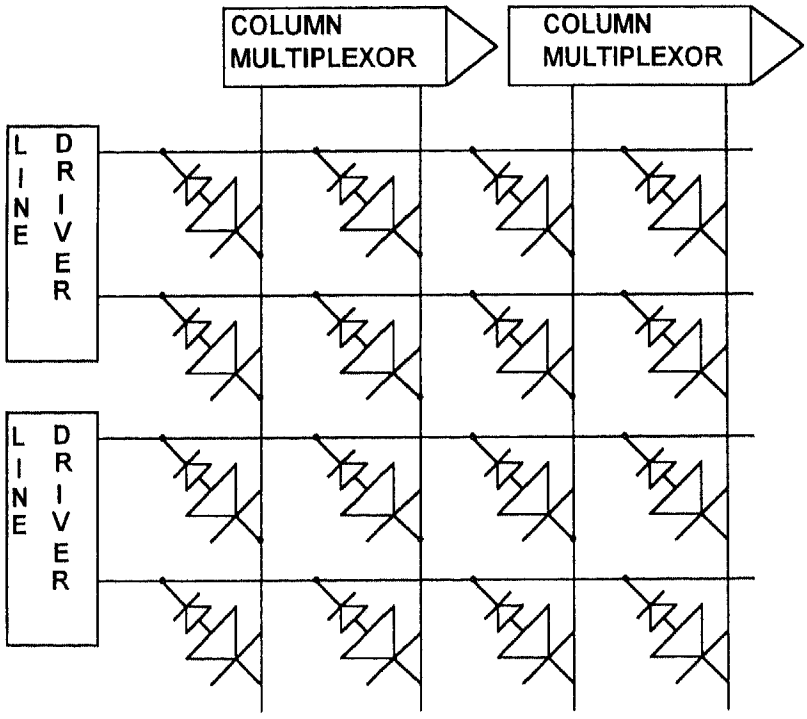

Fig. 1 : Block diagram of the detector

2.1. The aSi panel

A photograph of the pixel is given in Fig 2. The performances of the back-to-back diodes are optimized separately : the sD is a 20 x 20 μm^2 PIN diode with outstanding forward current characteristics (ideality coefficient of 1.8, degrading to less than 5 at 44mA/cm^2) combined with a leakage current of 10 nA/cm^2 at -4V ; the NiP photodiode is optimized for both low leakage (~ 1nA/cm^2) and high quantum efficiency in the visible range (>80% at 550 nm). Our current clean room facility and the fact that we used highly conservative design rules limited the fill-factor to 70%. This lead to a capacitance of the photodiode of ~ 1.9 pF ; 8 steps are necessary to complete the process.

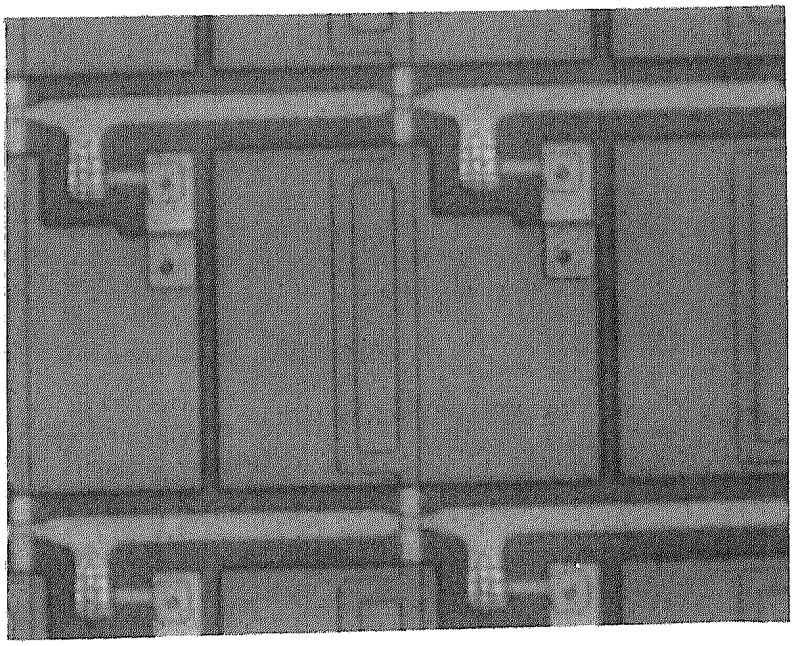

Fig. 2 : Microphotograph of the 2xD pixel

It should be noted that building a sD as the switching device is simpler than a TFT, and the intrinsic advantages of the 2xD process leads to possible impressive fill-factors (see section 4) ; the next step towards process complexity decrease is the use of a SLD processes ; this process is currently used for panels dedicated for radiography.

However, it should be pointed out that the 2xD pixel is more noise-sensitive to the 1/f noise of the switching device (sD) than the TFT/Diode pixel : Therefore, we have developed a very efficient diode deposition process which removes this 1/f noise and prevents the sD from late double injection mechanisms [8, 9, 10] (see results in section 3.6).

2.2. The scintillator

The conversion from X-ray to visible light is performed by a scintillator. We use a thin film (450 μm) of Cesium Iodide doped with Thallium CsI(Tl). As a matter of fact, this material provides both a high resolution and a high absorption (~70 %, see sections 3.1..3.3). This is attributed to the so-called 'needle' or 'pillar-like' structure of the material (which limits the lateral diffusion of the light) combined with intimate CsI(Tl) / panel contact.

2.3. Integrated circuits

Both row driver and column readout circuit are mounted on small PCBs linked via flexes to the panel by Anisotropic Conductive Film (ACF) techniques currently used in the Flat Panel Display technologies (Fig. 3).

The Row driver is a specific IC, with 120 outputs, low output impedance and including a grouping facility up to several MHz. The readout IC is also a specific IC designed in a CCD technology ; it consists in 120 charge sensitive inputs, several sensitivity ranges, analog memories and high speed output multiplexers ; its non-linearity performances in the highest sensitive range is below 1%, while its Equivalent Noise Charge is around : ENC ~ 1000 e- on a 100 pF load.

2.4. System electronics architecture

In addition to the custom IC driving electronics, the detector includes a fully programmable timing generator, a built-in 12 bit quantization running at 3Ms/s, a high rate fiber optic data link, and a system board.

Different operating modes can be downloaded by the main system (located > 10 m away) into the detector system board.

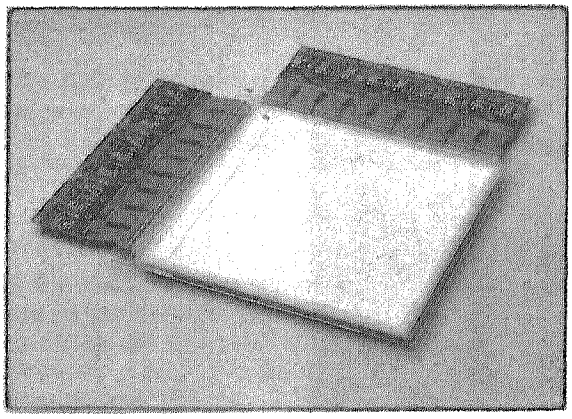

Fig. 3 : Panel equiped with its ACF-connected ICs

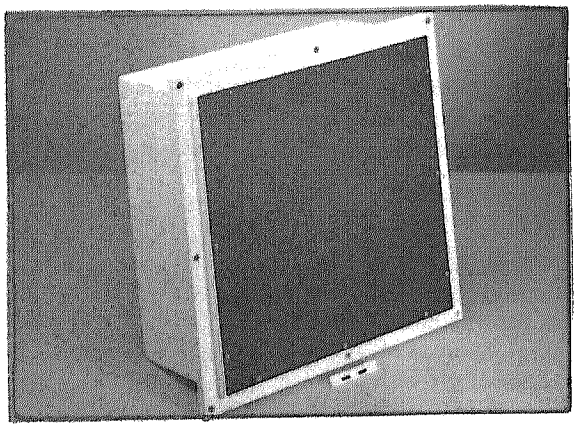

Fig. 4 : Detector housing : 280x280x146mm^3

2.5. Mechanical housing

A special attention was paid to the mechanical housing of the detector (Fig 4). This latter was then integrated in a clinical C-arm cardiology system ; it has been used extensively for months...

2.6. Main host system

The detector was linked to a powerful medical imaging system with on line and real-time specific data processing facilities.

2.7. Timing scheme (Fig 5)

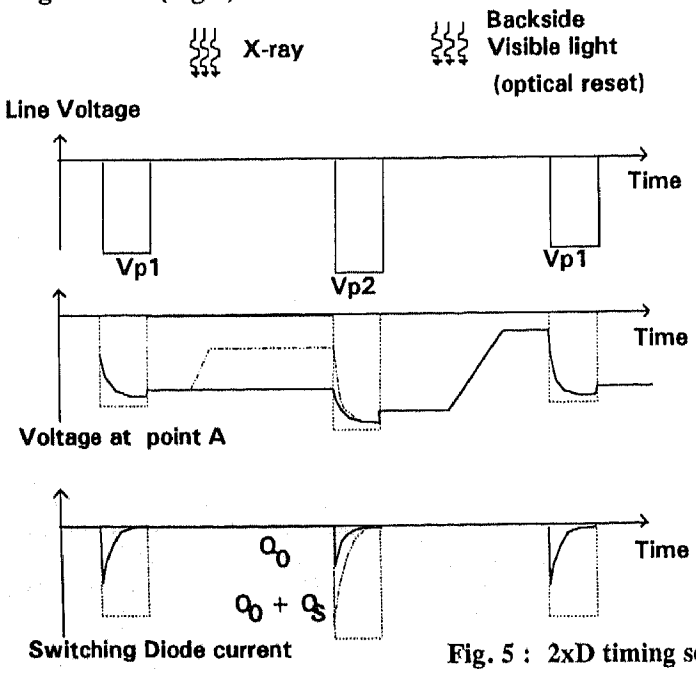

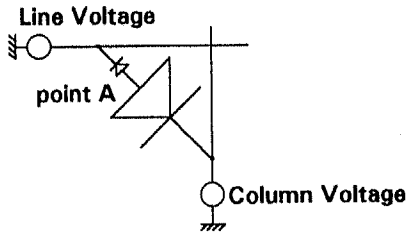

Fig. 5 : 2xD timing scheme

The 2xD pixel, while simple in terms of process steps, requires a dedicated timing scheme. It basically works as follows : During the readout period, the selected row provides a negative voltage (VP2) with respect to the column potential (which is grounded by the readout circuit) ; this turns the sD on and resets the photodiode capacitance. When the row is disconnected, both diodes are reversed-biased ; the photodiode can then be discharged by photocurrents originating from X-ray signals, and this amount of charge is detected during the next select pulse (next VP2) when the photodiode capacitance is re-charged back to its starting value.

However, the sD capacitance and almost voltage-dependent forward resistance, prevents from complete charging of the photodiode capacitance ; this mechanism creates lag and results in poor linearity especially for low signals.

Therefore, a bias charge is added by the use of a preset pulse (VP1) on all lines at the same time (during the frame preamble) ; the voltage difference between this preset pulse and the selection row voltage tunes the bias charge (typically : VP2-VP1 $\sim$-4.5- (-4) = -0.5 V).

Finally, an optical reset flash, applied on the panel backside, enables to drive the diodes common point towards a less negative value than the preset pulse voltage, and the frame can restart normally ; furthermore this optical flash saturates the deep traps in the aSi photodiode and therefore suppresses the so-called memory effects (see section 3.5). Highly linear and low noise performances can be reached which such a timing scheme, provided the convenient process is used for diode deposition. This is shown in the next sections.

3. DETECTOR PERFORMANCES

The detector performances as well as image quality has been evaluated in the various operating modes from low dose fluoro to high dose DSA. The available fluoro modes were 1024 x 1024 running at 12.5 f/s or 512 x 512 at 25 fr/s while the high dose mode was 1024 x 1024 at 6.25 fr/s.

The system doses ranged from 15 nGy up to 3 μGy ; min doses were assumed to be : min dose $\sim$ system dose / 3 ; thus, the minimum dose in low dose mode is around $\sim$ 5 nGy.

The photodiode reverse bias voltage was set to -3.5V for all modes ; this appeared to be a good starting value considering both reverse leakage currents and dynamic range.

However, consistent improvements regarding linearity, sensitivity and noise could be further reached by optimizing the modes individually.

3.1. Sensitivity

Photodiode optical detection efficiency : The photodiode quantum detection efficiency is measured on optical dedicated equipment : the detection efficiency as a function of wavelength is given in Fig 6 ; The diode was carefully optimized to detect more than 80% of the photons around 550nm which is particularly well adapted for our CsI(Tl) scintillator layer.

X-sensitivity : The X-sensitivity was measured under conventional conditions : 75 kV, 2 + 22 mm of Alu, the focal distance was 1m ; we assumed approximately 3E10 incident quanta / 1mm^2 for 1Gy . Both self-standing (grew separately and glued) and directly deposited CsITl layers (vacuum evaporation) were used ; thickness was 450 μm. In all cases, a white reflector was used. A sensitivity of **1150 e-/Xinc** (inc. fill-factor) was measured for both low and high dose modes ; taking into account an absorption coefficient of 70%, a fill-factor of 70%, we derive a photoelectric sensitivity of 2400 e-/abs X quantum.

We end up with a detector sensitivity (S) of : **S $\sim$ 1330 e-/nGy/pel** ; this is already a remarkable performance. However, the result may be markedly improved with suitable techniques as described in section 4.

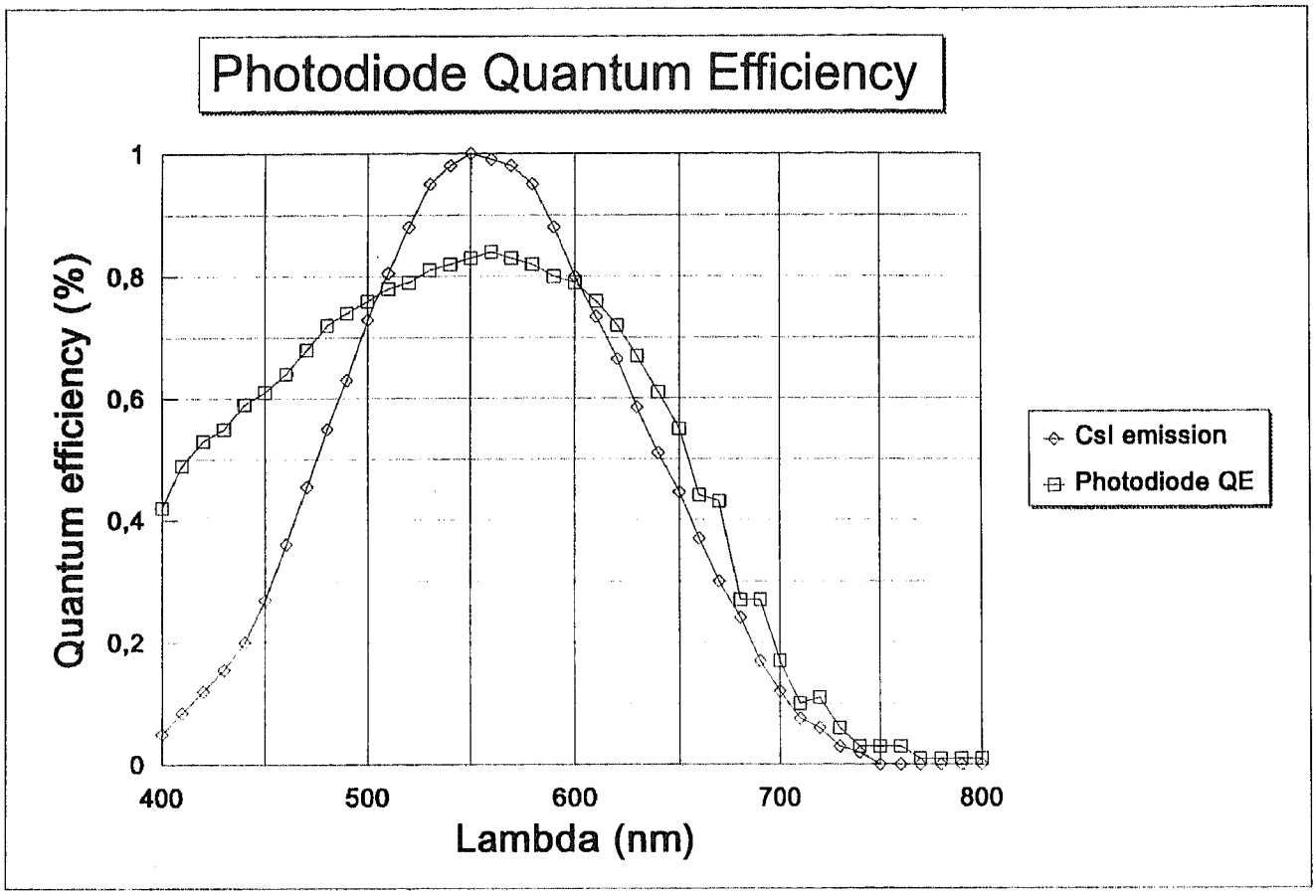

Fig. 6 : Photodiode quantum detection efficiency as a function of wavelenght

3.2. Linearity

Linearity is a key parameter non only for static applications, but also for dynamic ones ; Anyhow, we have measured this linearity in high dose because this mode is the most demanding in terms of dynamic range ; the doses ranged from 0 up to 18 μGy.

Our experience is that linearity errors are conditioned by the reverse bias voltage of the photodiode, which is not surprising [11] ; as a matter of fact, loading 18 μGy on a 1.9 pF capacitor, with a conversion factor of 1330e-/nGy/pel requires at least :

$$\text{Vbias} \sim 1330 \times q \times 18\,000 / 1.9E^{-12} \sim 2.0\,\text{V}$$

At Vbias = - 4V we found non linearity errors in the order of : 0.3 %.

3.3. MTF

Together with sensitivity and noise, MTF is a critical parameter ; the highest possible MTF below the Nyquist frequency is desirable ; however things may be not that easy and these 3 parameters have to be optimized with respect to each other.

To start with, we tried to enhance the MTF to the highest value ; the scintillator is CsI(Tl) with thickness of ~ 450 μm ; an efficient white reflector was used though it was not an advantage.

The measurement conditions are : X voltage = 50kV, no filtration, focal distance = 1m. The results are given in Fig 7. About 30 % are reached at 2 lp/mm (near 55 % at 1 lp/mm) ; at Nyquist frequency, more than 20 % are maintained. Moreover, the MTF from the scintillator alone (divide by the sinc function) gives MTF ~ 35 % at 2 lp/mm.

These values are considered as a breakthrough with respect to existing equipments. They could be further improved, when needed, by the use of a black (or no) reflector or by the use of a thinner layer ; this was not tried in this work.

We do think that these results are encouraging for both static and dynamic detector designs.

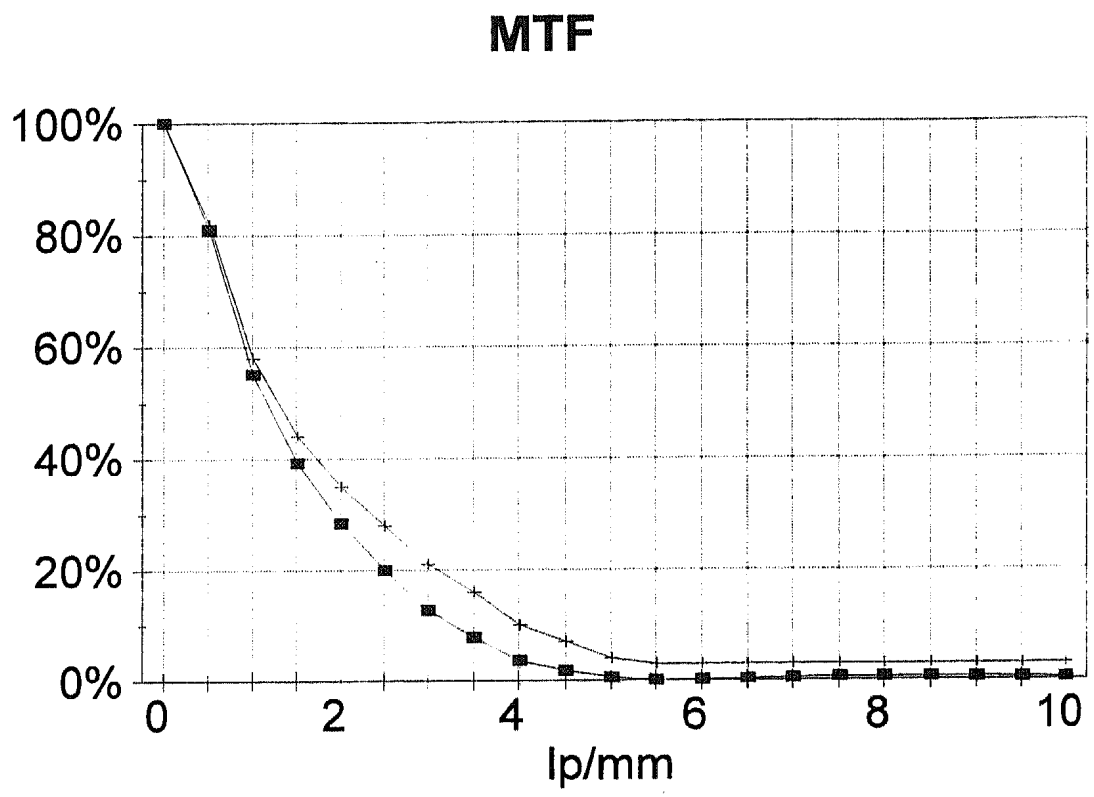

Fig. 7 : MTF measurement, global measurements (squares), and CsI(T1) extrapolated performances (+) ; white reflector

3.4. Coarse Contrast ratio

Coarse contrast ratio describes the ability of the detector to yield an image with a perfect dark region next to overexposed one. The conventional way of measuring it is a piece of thick lead whose surface is 10 % of the total field ; we took a circular one, placed it in the center of the field and measured profiles in both X and Y directions.

The X-ray conditions were the same as for the X-ray sensitivity measurement in high dose mode : at distances greater than 1cm from the transition less than 1 % of signal is noticed. Under the center of the discus, no residual signal can be measured. This is a considerable advantage of flat aSi detector over conventional XRII detectors for which coarse contrast of 10-20 are common (due to veiling glare). This was clearly pointed out by physicians, especially with phantoms' heads.

3.5. Image lag

As already mentioned in the literature, it is now agreed on that the lag and memory effects observed on aSi detectors is due to the amorphous silicon itself and not the scintillator screen nor pixel readout inefficiency : as a matter of fact, the pretty high density of states in the mobility gap is able, by itself, to create problems just by time-dependent trapping and detrapping mechanisms. Regarding this problem one can think at :

1. improving the material intrinsic quality,
2. saturating the deep states at each frame.

It is mandatory to push the material quality to its limits. Our experience is that highly optimized processes like ours yield a deep states density of around 3E15/cm3 which is state of the art.

The 2nd solution is realized by taking explicit advantage of the reset light which is required for the 2D driving scheme. This is not the case for TFT processes which required some adaptations. As a matter of fact, the reset light duration, shape and so on... are key parameters to optimize the lag, application by application : for example in fluoro modes, less than a few percents (at the first frame) are obtained without any problems.

However some difficulties occur in mixed applications and especially when a fluoro sequence is required immediately after a high dose exposition. In this case only, our detector, in its present status, did not reached the most severe specifications ; however, realistically non-zero switching times between a high dose applied and a fluoro sequence can be assumed which relaxes the problem of image lag. More over, some special erasing sequences, as well as digital processing algorithms are under evaluation.

3.6. Noise

The various noise sources contributions : The total noise finally measured in the detector originates from many sources that have to be optimized at the same time : some are theoretically incompressible (as the photodiode reset through a resistance, so-called KTC noise), some others depend on process/design performances trade-offs ; special attention should be paid to the readout IC whose process for fabrication, design, and driving scheme are essential. The following analysis is a detailed list of the major known sources .

The pixel : once addressed, the pixel behaves as a capacitor (the reverse-biased photodiode) reset by a directly-driven diode ; modelling the switching diode on-resistance using the conventional diode I(V) formula leads to a global noise of :

$$< e > \sim 400 \times \sqrt{2\, n/2 \times Cd},$$ expressed in electrons

In the formula, Cd stands for the photodiode capacitor, in pF; n stands for the ideality coefficient of the switching diode.

With n = 1.8 and Cd = 1.9 pF we end up with : $< e > \sim 750$ e-

Note : with non state of the art aSi deposition processes, some 1/f noise can be found ; if not carefully under control, this 1/f drastically degrades the pixel noise ...

Leakage currents : The leakage currents of both diodes contribute as shot noise in each pixel at the frame rate, and for all off-pixels connected to a given column, at the line rate. In our design, with If $\sim$ 1nA/cm² and 10 nA/cm² at -3.5V for the photodiode and switching diode respectively, the leakage contribution to total noise is estimated to less than 250 e-.

traps : In our design the contribution of traps is estimated to be linked with the active volume of the switching device ; we calculate a contribution in the order of 400 e-.

Readout IC : The readout IC is sensitive to the input capacitance with a slope of around 3 e-/pF. An offset value is measured which is due to the circuit intrinsic input capacitance. The current readout IC generation, integrated in the present detector, has a an offset of 650 e-. On 100pF capacitor it yields :

$$< e > \sim 650 + 3.1\ \text{e-/pF} \times 100 \sim 960\ \text{e-}$$

The next IC generation is already designed, fabricated and measured ; it markedly improves the offset value ($< e > \sim 300 + 3.5$ e-/pF), functionalities and ease of use.

The data line of the present detector is the column line ; it loads the IC with a capacitance of around 115 pF ; the capacitance is due to the detector column lenght (80%) and the number of pixels along the column (20%) ; the final noise contribution of the IC is :

$$< e > \sim 1010\ \text{e-}$$

Other contributions : There are some other noise sources than are not discussed in this paper (column resistance, analogue chain, A/D conversion)... They all contribute to around 600 e- in the current design.

Finally, the total noise is calculated to be : **$< e > \sim 1450$ e-**

Noise measurement methods : The noise level can be estimated using 2 different measurement methods ; both work on dark images :

Temporal measurement : In this approach, the noise is measured as the root mean square (rms) value of 1 pixel over time, and more precisely in this case, over 16 frames. In order to get rid of eventual line correlated noise, we in fact compute the rms of the difference of 2 neighboring pixels and correct the final value by $\sqrt{2}$. This makes the assumption that noise is white over frequency which is usually agreed on.

The statistics is computed over an Area of Interest (AOI), of 60 x 60 pixels ; defect pixels are eliminated via threshold adjustment while the likely rms is extracted by an iterative Gaussian fit algorithm. The major advantage of the method is that it works on rough non-corrected image, thus being insensitive to correction non-ideality.

Spatial measurement : The other way is to evaluate the rms residual spatial noise after all possible corrections : offset, gain, defects, and eventually line-correlated noise. It is hard to say at this stage, which method is faster ; the second one is more demanding but gives access to the noise power spectrum as described in [1].

Noise measurement results : Today, both methods end up with the same results of about 1500 e-. The obtained Gaussian histogram (summing all the AOIs over the full panel) is very sharp and repeatable (+-50 e-). This is in pretty good agreement with computed data and enables us to be confident in performance extrapolations.

3.7. Signal to noise analysis

Combining the signal at around 10 nGy (system dose for fluoroscopy) and electronic noise, leads to a S(10 nGy)/(Elec.Noise) ratio of ~18.2dB ; it is our experience that the incoming X-ray signal to noise ratio in the darkest areas of the image (minimum dose ~ system dose/3) should not be degraded by more than 10% by the detector. Taking into account this statement, the target for S(10 nGy)/(Elec.Noise) should be at least 23 dB ; this is in reasonable agreement with [12] ; we then derive that the present detector is suitable for system doses in the range 26 to 35 nGy.

Many short terms and medium terms improvements are possible, they are described in next sections.

3.8. DQE

The Detective Quantum Efficiency (DQE) has been measured for 10, 100 and 10 000 nGy doses (Fig.8). For the lowest dose (10 nGy) about 50 % are reached at 0-frequency while 10 % are maintained at 2 lp/mm.

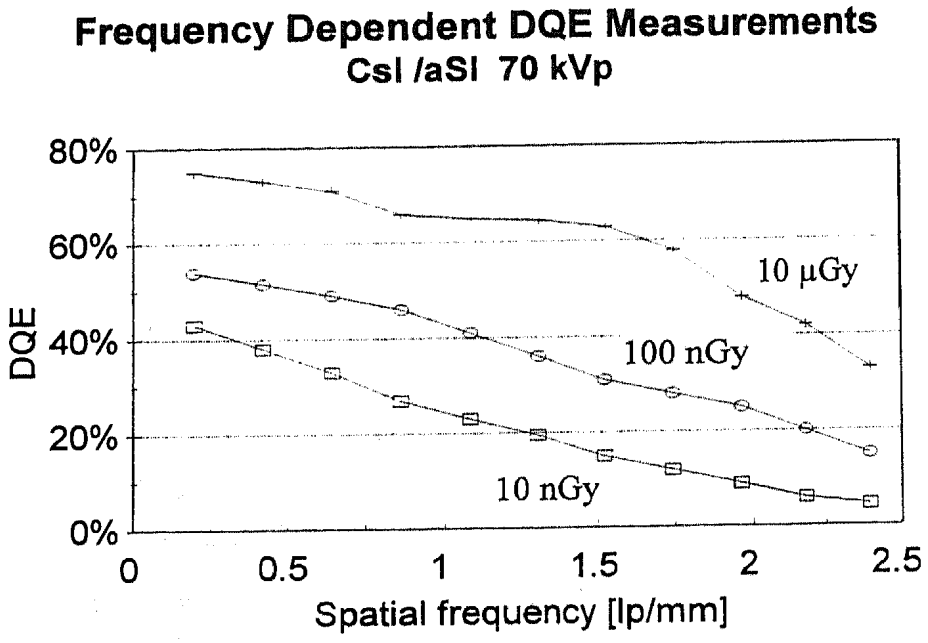

Fig. 8 : DQE measurements

3.9. Stability, X-ray hardness

Offset image stability with temperature : The detector temperature coefficient was measured to be approximately : -0.1 %/K ; these can be divided in : +0.2 %/K for the CsI(Tl) layer and -0.3 %/K for the aSi technology. These values are considered as acceptable as a continuous offset updating (much faster than likely thermal variations) is carried out in the detector.

X-ray hardness : Life doses of around 80 Gy where applied to the detector : an offset variation of 15 LSBs was noticed as well as a 10 % loss in sensitivity ; once again, these values are considered as acceptable because of continuous offset updating and periodic gain calibrations.

4. POTENTIAL PERFORMANCES OF LARGE AREA DETECTORS FOR DYNAMIC (FLUOROSCOPY) APPLICATIONS: DIODE VS TFT...

4.1. Possible short term improvement of the detector performances

Based on the performances obtained on the current detector, many sources of improvements can be thought about : the use of a state-of-the-art photolithography stepper opens the way to switching diode layout of ~ 10 x 10 μm associated with inter layer gaps of ~ 4 μm ; the use of the up-to-date generation of the readout IC (already available) as well as readout schemes, will significantly reduce the electronic noise ; moreover, some improvements in MTF/sensitivity trade-off can be easily reached : according to our calculations and combining all the improvements, signal to electronic noise ratios at 10 nGy in excess of 24 dB can be obtained, (noise levels of around 1000 e-, sensitivity in excess of 2 000 e-/nGy) which makes it possible to think about high performance fluoroscopy detectors.

4.2. Large area panel technology : 2xD vs TFT

It is our general conclusion to say that at the present stage of knowledge, 2xD and TFT/Diode processes are equivalent in terms of achievable results. Therefore the performances in pixel fill-factors, column capacitances, electronic noise, sensitivity at 10 nGy, and finally S(10 nGy) / (Electronic noise) have been estimated for both 2xD and TFT+ Diode processes ; the study was carried out on a 20 x 20 cm^2 field and for pixel size ranging from 200 μm down to 100 μm.

Assuming comparable design rules (4μm inter layer gaps, 10μm as minimum lines..) a minimum switching diode of 10 x 10 μm^2, and a minimum TFT design of 2x10/5 μm, the yielded fill-factors are clearly in favor of the 2xD diode process (88 % vs 78 % at 200μm, 75 % vs 53 % at 100μm) ; this only results from the intrinsic simplicity of the 2xD pixel construction (Fig9).

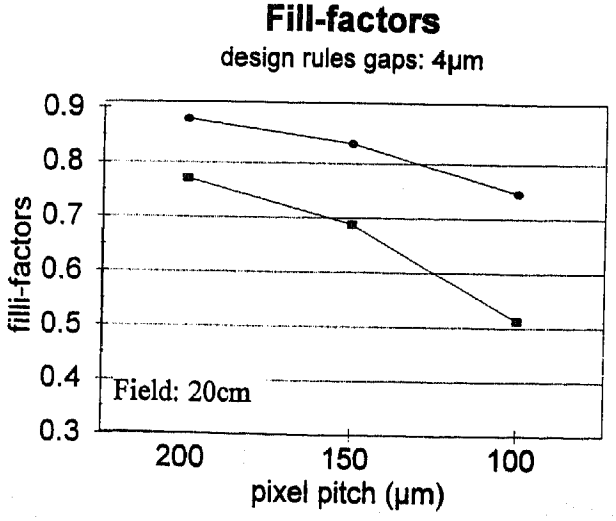

Fig 9 : fill-factor as a function of pixel size.

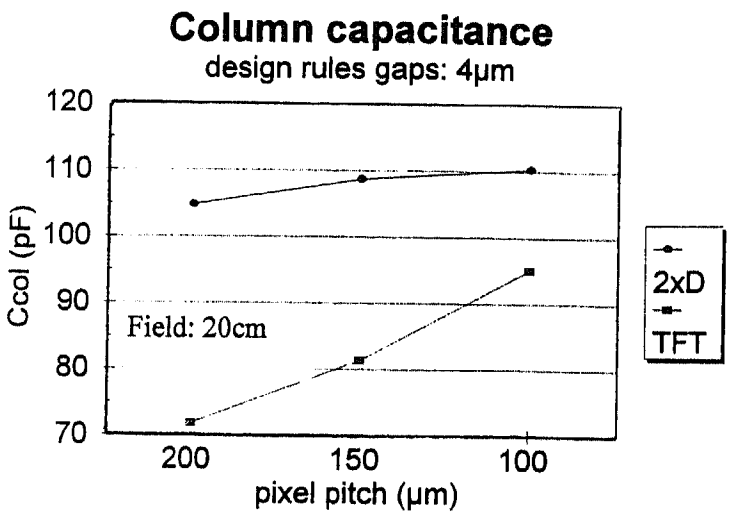

Fig 10 : column capacitance as a function of pixel size.

In terms of column capacitance, the TFT clearly leads the edge because of its poor fill-factor (~ 70pF are reachable with a filling factor of ~ 78% against 105pF / 88% for the 2xD) ; however, this advantage seems to vanish with decreasing pixel sizes (Fig10).

In terms of electronics noise, considering equal readout circuitry (our best available readout IC) and a frame rate of 30fr/s, the TFT is intrinsically better because of its poor fill-factor and associated low column capacitance (~1000e- vs 1200 e-). 800 e- may even be reached with a TFT if the fill-factor is further decreased (< 70%) (Fig11).

In terms of S/N, however, the conclusions are somewhat different (Fig12) :

- At 200μm, the S(10 nGy) / (Electronic noise) ratios are comparable : ~ 24 dB can be reached (that might be sufficient for both Card/Fluoro applications)
- At 150μm, the conclusions are comparable
- At 100μm, the 2xD has a 2 dB advantage.

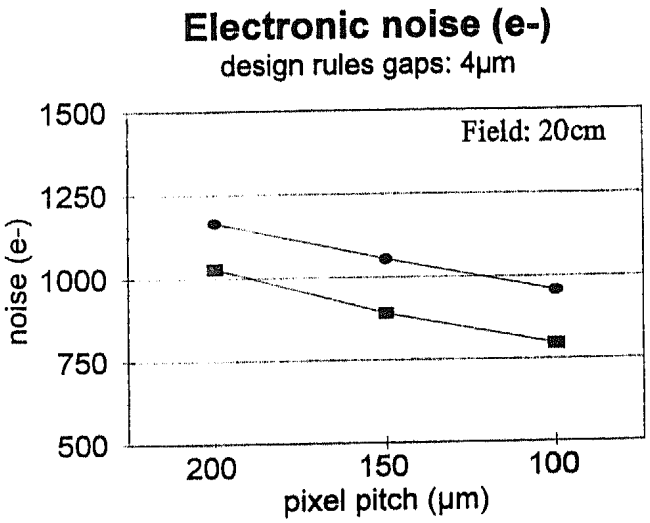

Fig 11 : 2XD vs TFT comparison : noise

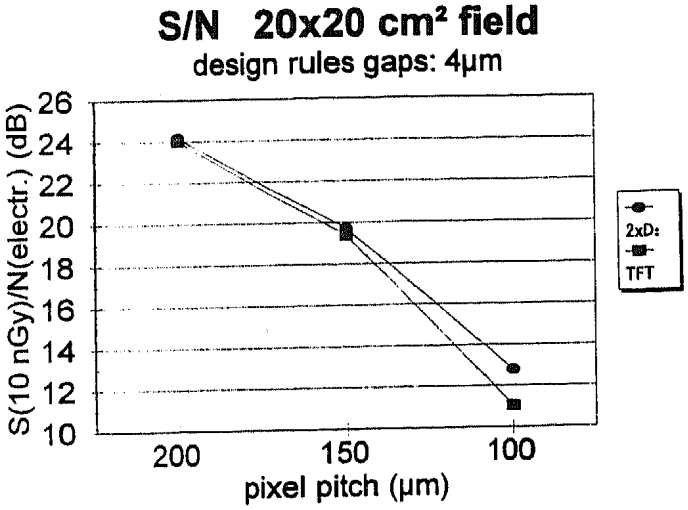

Fig 12 : S (10 nGy)/Elec. noise ratio.

5. CONCLUSION

Experimental results in the laboratory show that the parameters which define the image quality are comparable to II.TV systems.

After first experience in the clinical environment, the users emphasized, especially in digital cinema, the high contrast and the brilliant image impression.

In fluoroscopy mode, the detector must be further improved in terms of S/N ratio in order to compete with both the continuously improving XRII-TV systems (especially with the introduction of excellent CCD sensors) and the irreversible trends to dose reduction.

It is our feeling that these improvements are possible thanks to both state of the art equipment (making it possible to drastically increase the fill-factor and consequently, the sensitivity) and high performance readout ICs.

For fluoroscopic imaging, both TFT and diode processes are good candidates to built up large area (~ 40 x 40 cm²) full-spec fluoroscopy detectors.

As for high resolution radiography and mammography detectors, the superior fill-factor as well as intrinsic simplicity of single layer diode based processes make them definitely promising.

6. ACKNOWLEDGMENTS

This project was supported in part by EUREKA grant EU 651 under the name ASTRID, and by the french department of industry.

We thank all the people who contributed to experimental set up and data acquisition in both TTE and SIEMENS.

7. REFERENCES

1. U. Schiebel & al, Philips Research Lab, "Fluoroscopic X-ray Imaging With Amorphous Silicon Thin Film Array " SPIE 94.
2. R.A Street and L.E. Antonuk , Xerox, "Amorphous Silicon Arrays Develop A Medical Image", IEEE circuit and Devives july, 1993
3. V. Perez-Mendez & al, Lawrence Berkeley Laboratory, " Amorphous Silicon Pixel Radiation And Associated Thin Film Transistor Electronics Readout " Electrochemical society thin film transistor technologies symposium, Miami Beach Florida Oct-9-14, 1994
4. Lothar S. Jeromin, Denny L.Lee, E. L. DuPont de Nemours & Co, " A Direct Radiography System for the Future", Computer assisted Radiology'95, juné 21-24, 1995.
5. N.C Bird, C.J Curling C. van Berkel, Philips Research Lab, " Large-area Image Sensing Using Amorphous Silicon nip Diodes", Elsevier Science, Sensors and Actuators, 1995
6. C. van Berkel, & al, Philips Research Lab, "Physics of a-Si:H switching diodes", 15th International Conference on Amorphous Semiconductors Cambridge (UK) 6-10 september 1993.
7. Hidenori Mimura & al, Nippon Steel Corporation, " A Two-Dimentional Image Sensor With a-Si:H pin Diodes " Elsevier Science Publishers, Applied surfece Science, 1991
8. M. Hoheisel & al, Siemens AG, " Physical aspects of a-SiH image sensors" Elsevier Science Publishers, Journal of Non-cristalline Solids , 1990
9. R.A.Street & al, Xerox, "Physics Of Double Injection Transients In Amourphous Silicon p-i-n Diodes", Journal of Applied Physics, 15 september, 1992
10. B. Yan & al, "Experimental Study Of Forward Current Transients In Amourphous Silicon p-i-n Structures", Applied Physics Letters, 31 October, 1994.
11. J. Yorston & al, Xerox, "Photoreponse Linearity Of a-Si:H Imaging Pixels",MRS Spring meeting, 1993
12. Hans Luijendijk, Philips Med. Systems, "Practical experiment on noise perception in noisy images" SPIE 94